Paper: ASAT-14-225-ST

14th International Conference on
AEROSPACE SCIENCES & AVIATION TECHNOLOGY,
ASAT - 14 – May 24 - 26, 2011, Email: asat@mtc.edu.eg
Military Technical College, Kobry Elkobbah, Cairo, Egypt
Tel: +(202) 24025292 –24036138, Fax: +(202) 22621908

Thermo-Structural Analysis of Combined-Wall Nozzle

A.R. Gomaa*, H. Kamal†, and M.A. Al-Sanabawy‡

Abstract: In this work, investigation of the thermo-structural response of steel-composite rocket nozzle is carried out using the finite element method; in the form of commercial package ANSYS. A validation of ANSYS for thermal and structural analysis is done first for simple problems, then the analysis done with the nozzle. The result of thermal analysis shows that thermal loads have a great effect in generating a huge amount of stresses on the nozzle structure (more than 60% from the total stresses on the nozzle). The convictive heat transfer coefficient has a great effect on the temperature transferred to the nozzle wall. The composite material resists temperature augmentation, so it is regarded as a thermal protection material.

Keywords: thermo-structural analysis, steel-composite nozzle.

1. Introduction

A solid rocket motor nozzle is a carefully shaped aft portion of the thrust chamber that controls the expansion of the exhaust products so that the energy forms produced in the combustion chamber are efficiently converted to kinetic energy. Nozzle design is an iterative process in which aerodynamic, thermodynamic, structural, and fabrication considerations are manipulated within the constraints to produce a preliminary nozzle configuration. Metals are the basic structural materials of rocket motor (RM) nozzles used for many decades. Composite materials are used instead of conventional materials. This is because of superior material properties of composites over metals.

The objective of the thermal design phase is to maintain nozzle aerodynamic contour design and to limit the temperature of the structure to acceptable levels. The structural mechanics design objectives are to configure the basic structural framework that will assist the applied loads and supports the insulators and liners to carry the nozzle loads.

The finite element method (FEM) has emerged as an important and valuable tool for decades to design and analysis of aerospace structures. One of the most common FEM codes is ANSYS, which is a comprehensive general-purpose finite element code. In this work, ANSYS is used for analyzing the RM nozzle made of conventional and composite material.

In this work, the thermo-structural analysis of steel-composite rocket nozzle is carried out. The analyzed nozzle consists of 3 main parts (steel-composite material-graphite insert for throat) loaded internally thermally and mechanically by temperature and pressure produced from combustion gases. The nozzle prevent from moving in all directions at the conjunction with the motor case. The firing duration is 7 seconds and the following assumptions are considered:

* M.Sc. student, Egyptian Armed Forces.
† PhD, Egyptian Armed Forces.
‡ Assoc. Prof., Egyptian Armed Forces.

1- The bonding between materials is perfect.
2- The composite material properties only do not change with temperature.
3- The radiation effect in thermal analysis is neglected.
4- No large deflections in structure.

A variety of recent works account for the growth in knowledge and techniques in the assessment of the thermo-structural behavior of (SRM) nozzles. Mukherjee and Sinha [1] used the finite element method to analyze the thermo-structural behavioral of rotationally symmetric multidirectional fibrous composite structures; a typical uncooled convergent-divergent nozzle is analyzed for a couple of advanced composite materials. A. Zayed [2] built a finite element code for thermal and structural analysis of axisymmetric rocket nozzles made of composite materials with non-linear thermal and mechanical properties. A case study is chosen to be analyzed using the built code. The efficiency of the built code had been proven by the good agreement with results obtained from the validated finite element code, MARC, and from experimental results. E.V.Morozov, and J. Beaujardiere [3] illustrates the uncoupled dynamic thermo-structural response of a composite rocket nozzle throat. All thermo-structural analyses are performed using the commercial finite element program ADINA. . It is shown that for the region of the composite nozzle investigated, the dynamic thermo-structural solution oscillates closely about the quasi-static solution. It is also observed that there exists a wide range of variance in maximum stress magnitudes predicted by either solution – ranging between 0.28% and 137% – and that, in general, the degree of variance is significant. Francisco Alhama, Antonio Campo [4] introduces a robust computational technique named the network simulation method (NSM) that is exemplary for the numerical prediction of spatio-temporal temperatures in multi-layered composite walls in regular coordinate systems, The problem that was analyzed here deals with a composite nozzle wall of an experimental rocket engine that is fabricated with tow dissimilar materials: a metallic substrate and a ceramic coating. Chang and Kutlu [5] made an investigation to study the strength and response of cylindrical composite shells subjected to out-of-plane loadings undergoing large deformations. Analytical model is developed to predict the mechanical behavior of structures from initial failure, through post failure to final collapse. A nonlinear finite element code based on the updated Lagrangian formulation was developed for the model. Tsung-Chien Chen, and Chiun-Chien Liu [6] offered an effective analytical method for thermal-protection layer design in the solid rocket motor by simulations of the measured temperature on the nozzle throat-insert outer surface to estimate the heat flux in the inner wall on-line with accuracy, An 0n-line methodology, based on the input estimation method including the finite-element scheme, was developed for estimating unknown input heat flux on the boundary. The transient thermo-structural response of a composite rocket nozzle employing a thin protective layer was predicted using finite element analysis by Vandenboom and Heister[7], and an assortment of structural and thermal results are presented for both the substrate and the protective layer. Cozart and Hsivakumar [8] performed a finite element axisymmetric stress analysis of a 3-D braided perform ablative composite rocket nozzle, incorporating a material ablation model. In the work of Yoo et al. [9], a kick motor nozzle utilizing spatially reinforced composites was subjected to finite element thermo-elastic analysis following the development of a material model used to homogenize various spatial reinforcement architectures. Kumar et al. [10] undertook an extensive thermo-structural analysis of composite structures, incorporating temperature dependent properties, and thermal, thermo-chemical and mechanical loads, and subsequently performed a coupled thermo-structural stress analysis of an SRM nozzle comprised of various orthotropic and isotropic materials.

The finite element method is used to investigate the thermo-mechanical analysis of a combined steel-composite nozzle. A validation of ANSYS for thermal and structural

analysis is done, first, for simple problems, then the analysis is carried out on the nozzle. The thermal and structural results are discussed for the instants of 1 and 7 seconds from firing duration, and final conclusions from these results analyzed.

2. Validation of the ANSYS Finite Element Code

Before any significant thermo-structural analyses were conducted using ANSYS, a validation and assessment procedure was carried out to establish the thermo-structural capabilities of the program. In essence, the procedure involved the comparison of results numerically derived by ANSYS, to those obtained from an analytical solution for a problem as reflective as possible of the geometry and material architecture, featured by composite SRM nozzles in general.

2.1. Stress Analysis of Hollow Cylinder Under Structural Load

This sample problem is a simple configuration to be used for verification of stress analysis of ANSYS compared to the analytical solution **[11]**.The model of sample problem is shown in Fig.1, which represents a simple ring loaded by pressure on its internal surface.
The material of this model has Young`s modulus E = 1.E+7 and Poisson`s ratio ν = 0.3, the applied pressure has the unit value. The ring is clamped at y=0 and y=0.2
The results are compared with the exact solution as illustrated in Table 1.

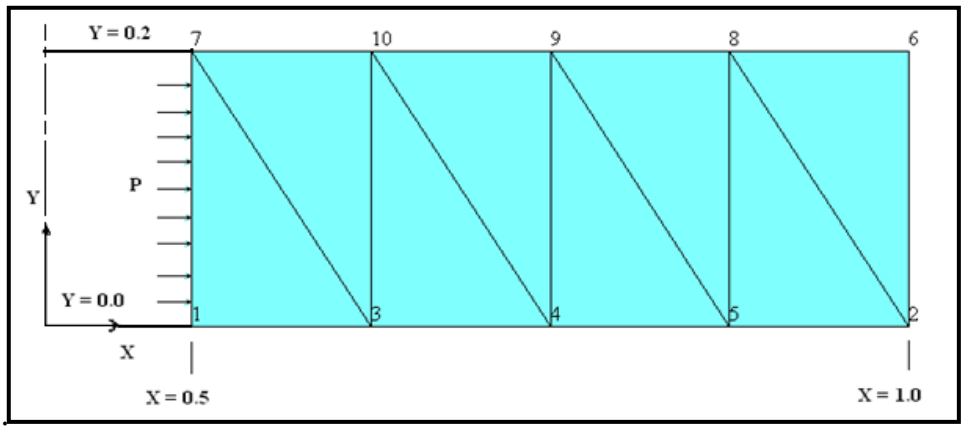

Fig. 1 Model of stress analysis for the sample problem

Table 1 Comparison of results of ANSYS and analytical solution [11]

X		ε_x	ε_z	σ_x	σ_z
0.5	ANSYS	-0.15579E-06	0.19044E-06	-0.99845	1.6648
	Analytical	-0.1560E-06	0.19066E-06	-1.00000	1.66666
0.625	ANSYS	-0.93512E-07	0.12818E-06	-0.51935	1.1859
	Analytical	-0.9360E-07	0.12826E-06	-0.52000	1.18666
0.75	ANSYS	-0.59665E-07	0.94332E-07	-0.25895	0.92564
	Analytical	-0.5970E-07	0.94370E-07	-0.259259	0.92592
0.875	ANSYS	-0.39246E-07	0.73916E-07	-0.10187	0.76860
	Analytical	-0.3926E-07	0.73931E-07	-0.102040	0.76871
1.0	ANSYS	-0.25989E-07	0.60660E-07	0.1082E-03	0.66664
	Analytical	-0.2600E-07	0.60666E-07	0.000	0.66666

2.2. Transient thermal stress analysis

This problem is a thick cylinder heated by convection on the internal surface Fig.2. Boundary conditions and material properties were selected such that an exact analytical solution is obtainable for comparison **[13]**. Convection at internal surface takes place from a fluid having bulk temperature of 373 K. results is calculated during time of 200 sec by incremental time steps.

The model is discretized into finite elements as shown in Fig.2. The model consists of 231 nodes and 200 elements.

- **Material properties :**

Table 2 Material properties for sample problem [12]

Item	value	unit
Density	7850	Kg/m^3
Specific heat	410	J/kg.k
Thermal conductivity	60.5	W/m.k

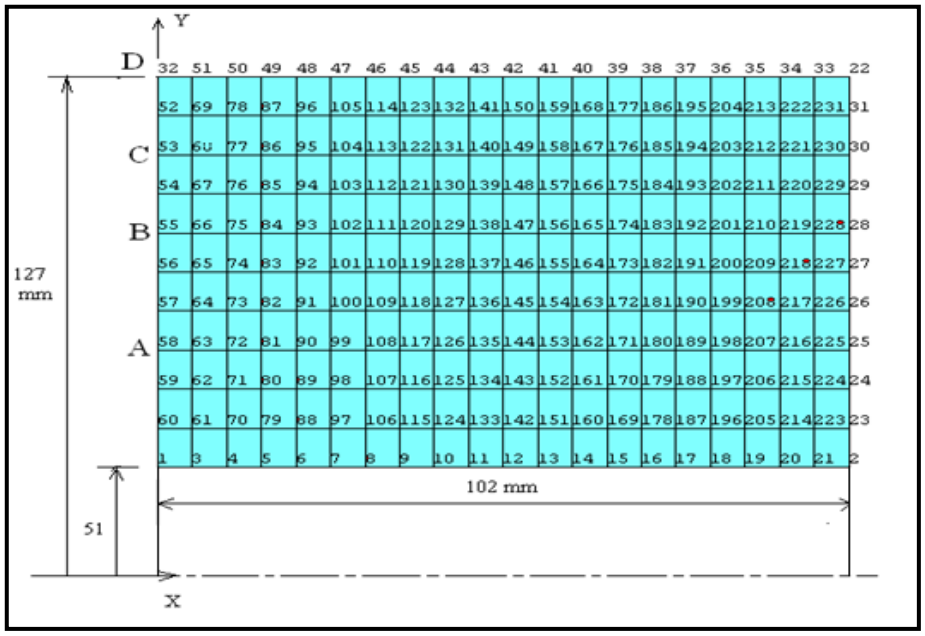

Fig.2 Model of the sample problem: dimension & discretization

Boundary conditions:

This model is fed by bulk fluid temperature of 373 k at its internal surface; the structure has initial (reference) temperature of 273 k. The forced convective coefficient is 864.7 $W/m^2.k$

Time steps:

The time interval from 0 to 200 seconds is divided into incremental time steps. Three different time steps are used in this problem; 5,10and 20 seconds.

Results:

The output of the transient thermal analysis is nodal temperature at each time step. Temperature-time curve at certain node depends on the time steps. Figure 3 shows the history changes in the temperature of a node on the external surface due to change of incremental time. In this case it is observed that the smallest increment of time (5 seconds) has given smaller error compared to analytical solution.

The temperature history of the external surface obtained as output of ANSYS is compared to the analytical solution as illustrated in Fig.4. Agreement of results indicates the efficiency of ANSYS.

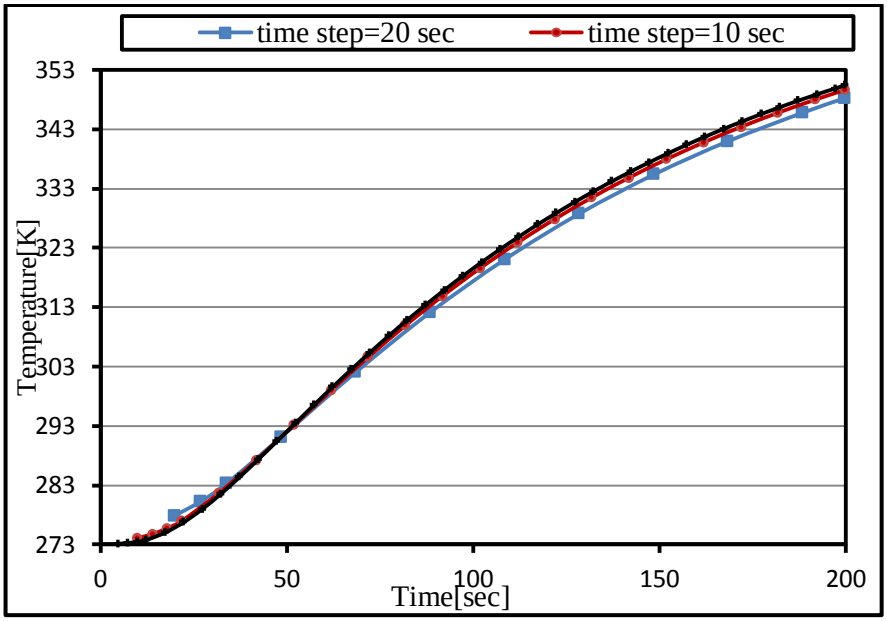

Fig. 3 Temperature history on the external surface for different incremental times

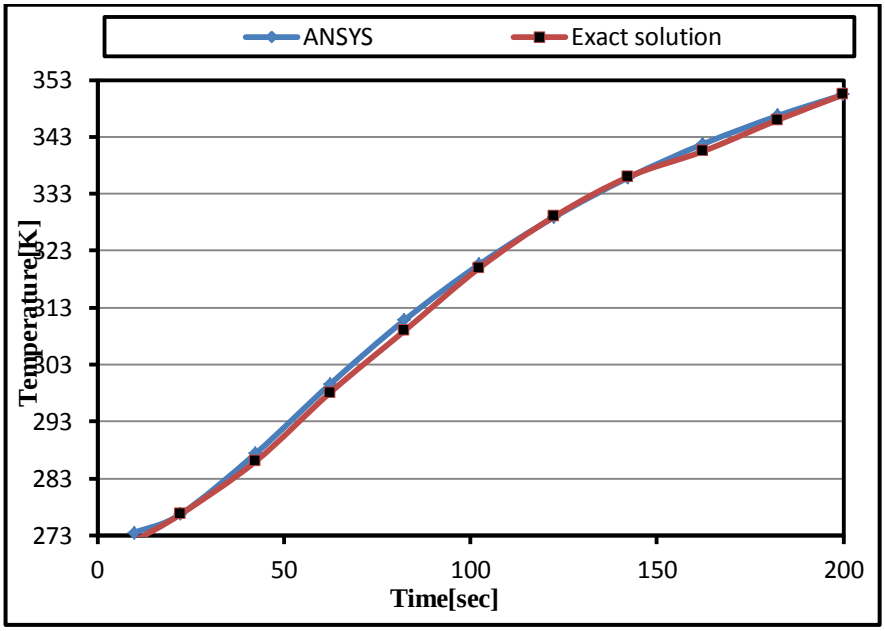

Fig. 4 Exact and ANSYS solutions of the sample problem for time step=5s [50]

It is clear that, the rate of increasing of temperature changes due to nodal radial coordinate. Figures5 and 6 Show that the difference between the internal surface and external surface temperatures decreases by time increasing, this means that, the temperature gradient decreases through the time interval.

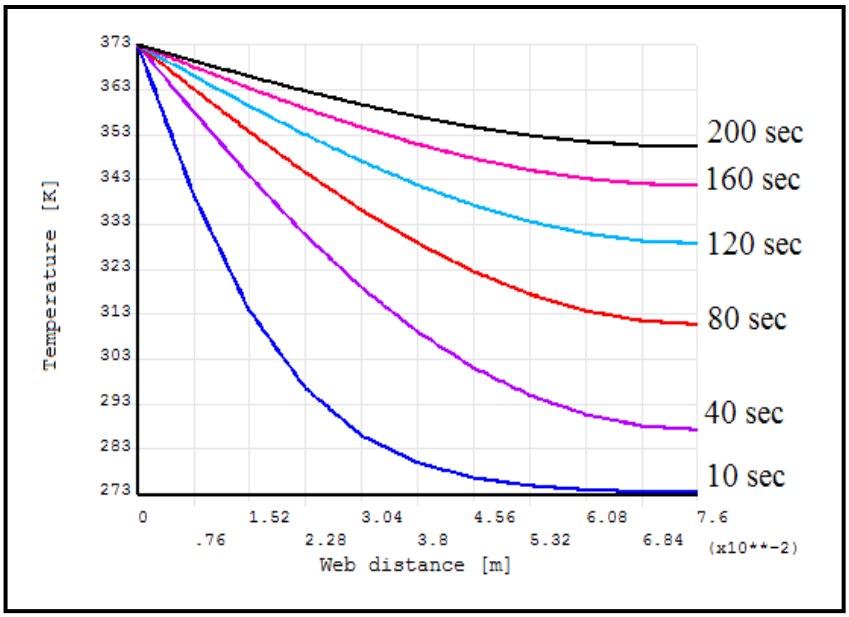

Fig. 5 Temperature history across the web through the total time (200 s)

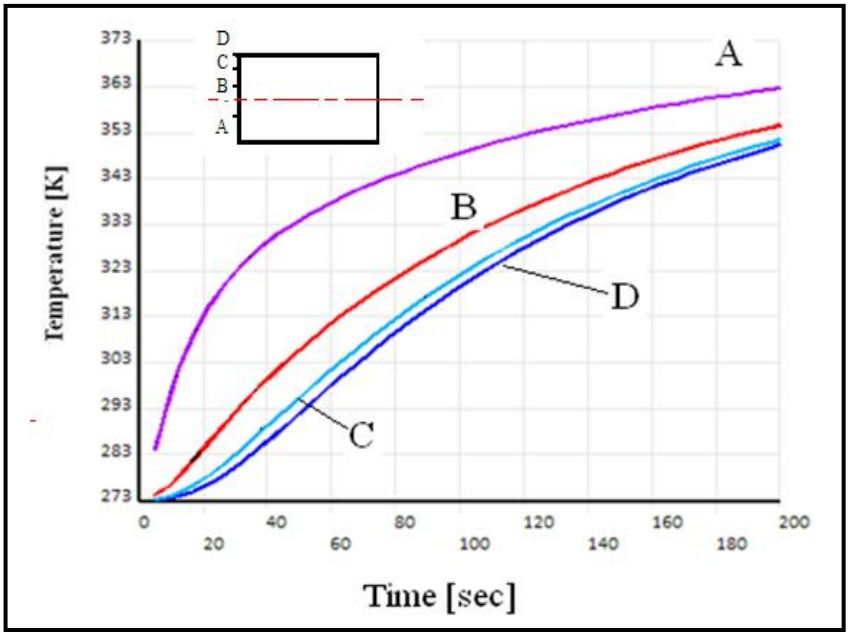

Fig. 6 Web nodal temperature through the total time interval (200 s)

3. Combined (Steel & Composite) Nozzle Model

Thermo-structural analysis is done on the nozzle shown in Fig.7. The nozzle consists of three substructures namely the Integral Throat e (IT) made from graphite, the composite material (Superaplast) insulator – which isolates the steel, and the main steel structure. The nozzle total length is 210 mm, with a throat diameter of 27.8 mm, and an expansion ratio of 6.89. The nozzle applied to loads from combustion gases, the variation of these loads along the nozzle is shown in Fig.8.and Fig.9.as a function of axial distance from the entrance point, respectively. These loads obtained from thermo-chemical calculations done for this nozzle with input data for the propellant used in this motor, the output from thermo-chemical calculations are temperature and pressure along the nozzle axes.

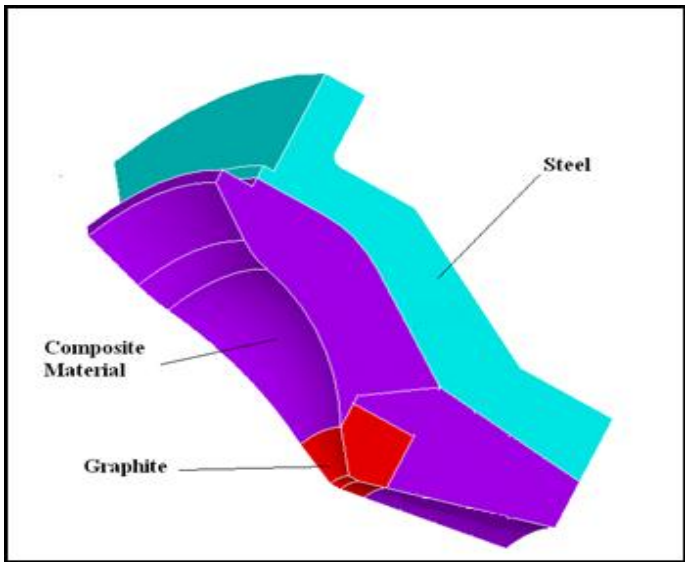

Fig 7 3-D geometrical model for the nozzle

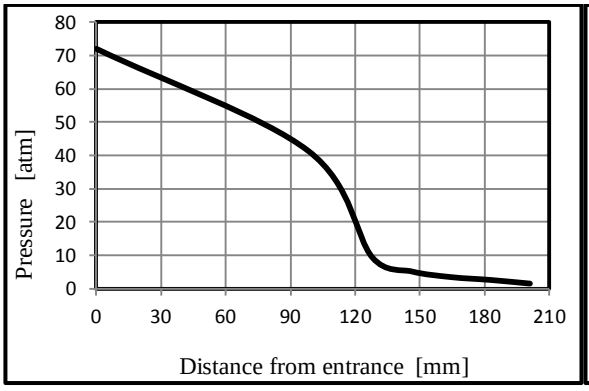

Fig.8 Pressure along the nozzle

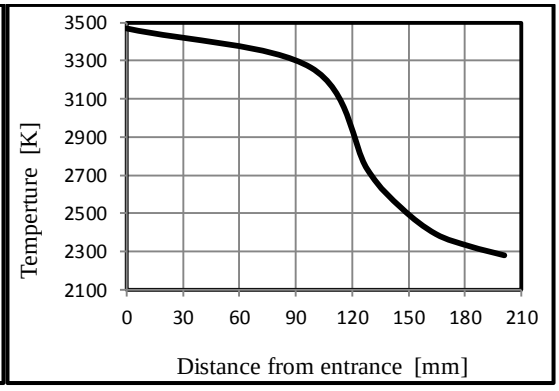

Fig.9 Temperature along the nozzle

3.2. Material properties, loading conditions and the nozzle FE model

Owing to the rotational symmetry of the geometry, loading conditions and materials being employed, the choice of performing axisymmetric thermo-structural analyses was a natural one, and led to time and resource efficient computations. Material properties of the three substructures, shown in Table 3, were taken to be temperature independent as a simplifying assumption [4]. The associated principle orthotropic directions correspond to a cylindrical coordinate system where r, θ, and z are represented by 3, 1, and 2 respectively. The parameters E_{11}, E_{22}, E_{33}, G_{12}, G_{13}, G_{23}, ν_{12}, ν_{13}, ν_{23}, k_1, k_2, k_3, α_1, α_2 and α_3, are the moduli of elasticity, shear moduli, Poison's ratios, thermal conductivities and coefficients of thermal expansion in their associated directions respectively, whilst C_p and q are the materials' specific heat capacity and density respectively. The thermal and pressure loading data applied in all analyses of the composite nozzle were obtained from the experimental data from a static firing test of the nozzle.

For modeling the designed nozzle,(in thermal analysis) the 3-D 10-node tetrahedral thermal "solid 87" element was selected from the ANSYS computer program element library to the steel (material no.1) and the 3-D 20-node thermal "solid 90" element selected for the

composite (material no.2), and (in structural analysis) The 3-D 10-node tetrahedral structural "solid 187" element was coupled with thermal element "solid 87" to the steel (material no.1) and the 3-D 20-node structural "solid 186" element was coupled with thermal element "solid 90" for the composite (material no.2). The nozzle was divided to 8 volumes at which the temperature and pressure varied along x-direction from the inlet to the outlet of the nozzle. The model was discretized into 16552 element and 25477 nodes.

In order that the two models become identical for the solution of the coupled problem, the discretized model formerly used for heat analysis must be used and the thermal distribution from the thermal analysis used as an input for the structural analysis.

The analysis of the nozzle considers a zero displacement in the axial and radial directions X and Y at the interface with the motor case. The calculated pressure is multiplied by 110%-120% to obtain the value of the maximum expected operating pressure MEOP. The effect of temperature on the structure is studied at chosen time instants (1sec) at the beginning of firing test, and at (7sec) at the end of burning time. The 3-D discretized model is shown in Fig.10. Three paths are taken at the finite element model to carry out the analysis at the three different sections (entrance, throat, and exit); this is shown in Fig.11.

Table 3.Consititutive material properties for the nozzle at room temperature

Value	Graphite	Composite	Steel
K [w/m.k]	k_x = 121.1 k_y = 69.2	k_x = 0.5 k_y = 0.3	60.5
C [J/kg.k]	1046	1000	420
ρ [kg/m^3]	1750	1850	7850
E (GPa)	E1=5.1713 E2=6.2055	E1=60.67 E2=24.82	200
ν	ν_1=0.23 ν_2=0.02	ν_1=0.24 ν_2=0.49	0.3
α (1/^{o}K)x10^{-6}	α_1=2.7 α_2=3.96	α_1=6.3 α_2=20.52	12
X(GPa)	0.031	1.289	1.241
X`(GPa)	0.062	0.821	1.241
Y (GPa)	0.021	0.0462	1.234
Y`(GPa)	0.069	0.174	1.234
S (GPa)	0.021	0.045	0.752

3.3. The solution procedure

As outlined previously, the composite nozzle structure is subject to both mechanical and thermal loads during the period of analysis. To develop a solution to such a thermo-structural problem, the ANSYS finite element code employs a two stage solution scheme using a thermal and mechanical model of the problem, which results in an uncoupled thermo-structural solution. The technique is applicable to both transient (thermal) and static (structural) analyses, and the first stage entails the analysis of the thermal model, using ANSYS's thermal module. This analysis allows the temperature distribution in the nozzle as a function of time – required by the structural model to determine the thermal strains generated by thermal loading – to be established. In the event that the thermal and structural model

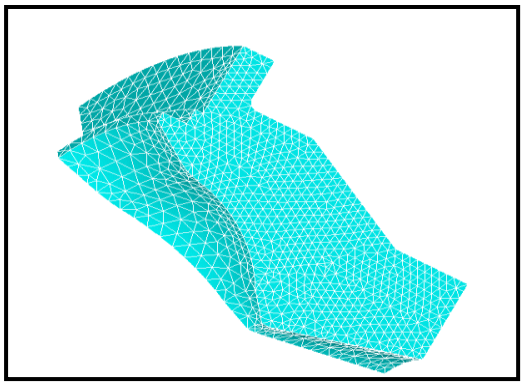

Fig. 10 Nozzle discretization

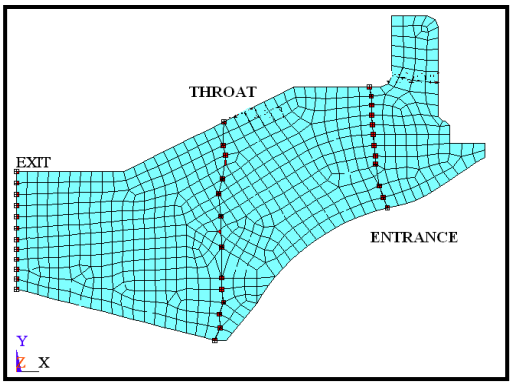

Fig. 11 Entrance, throat, exit sections

meshes, and solution time step formats are equivalent – such as in this case – ANSYS reports this temperature distribution by writing a temperature file to memory, with this temperature file linking the thermal analysis to the structural analysis–the latter being the second stage of the thermo-structural solution procedure. The structural model, featuring all associated mechanical loading, is then instructed to read the appropriate temperature file, and during the subsequent structural analysis, a temperature input for each node in the model is copied at each time step of the analysis. In this way, the second analysis is able to account for the effects of both the thermal and mechanical loading, and thus generate a thermo-structural solution. Regarding this solution procedure however, it should be noted that the resultant Thermo-structural solution is an uncoupled one. That is, the thermal field has an effect on the stress/stain field, but no facility is made available for the stress/strain field to influence the thermal field in return.

4. Results and Discussion

4.1. Thermal analysis results

The nozzle was subjected to thermo-structural loading for 7 seconds with incremental time step for the calculation 0.05 second. The temperature distribution in the wall thickness at time = 300 second is shown in Fig.12. The temperature distribution resulting from the calculation of heat transferred to the nozzle wall at different sections and times (exit and throat) are shown in Figs.13, 14.

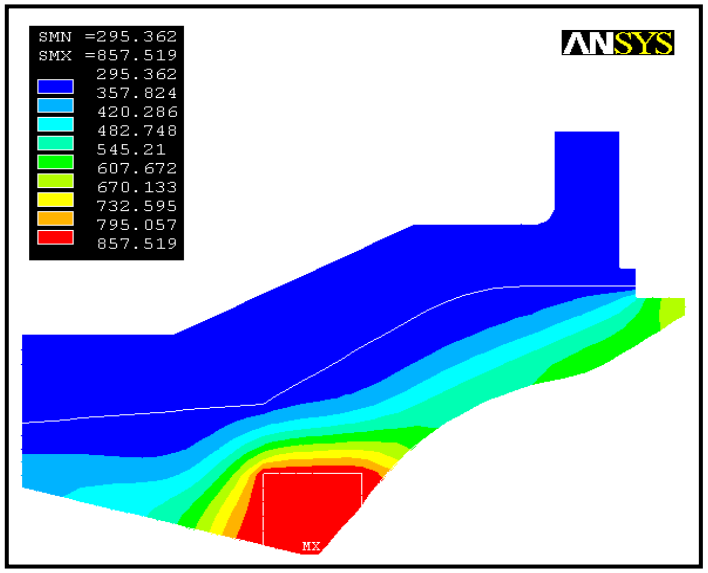

Fig. 12 Temperature distribution at time (3 s)

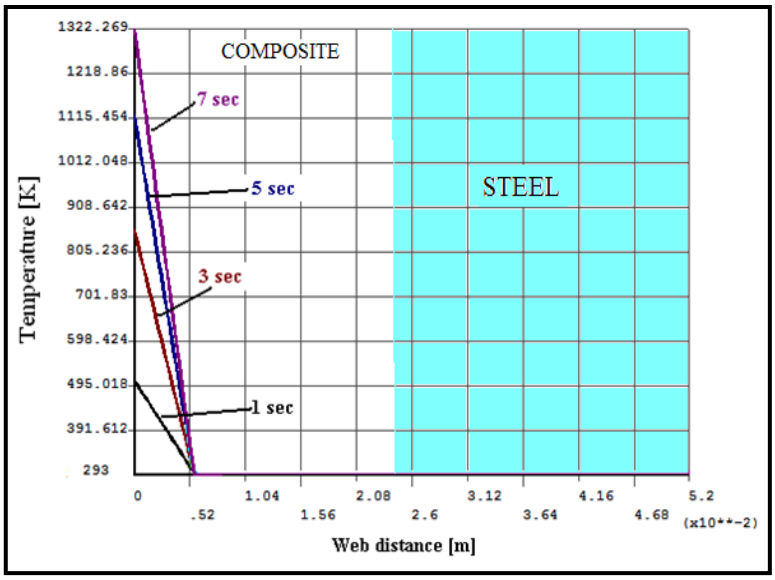

Fig. 13 Temperature history across the web thickness at exit

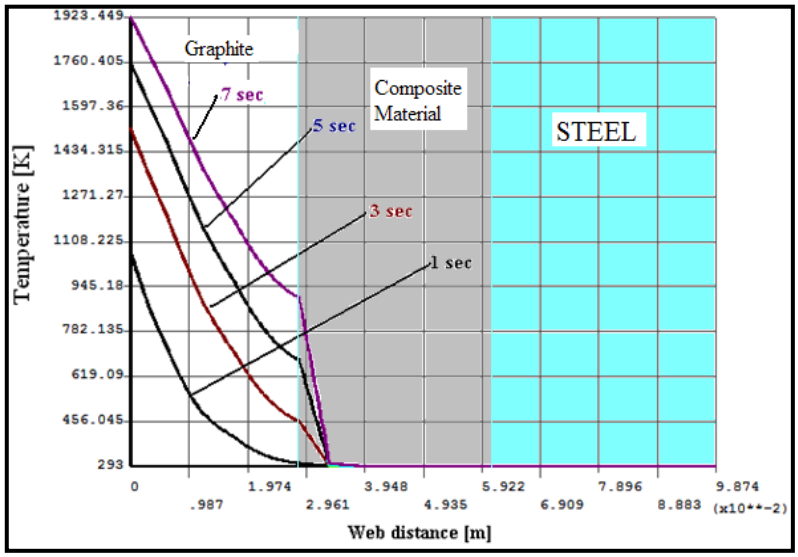

Fig.14 Temperature history across the web thickness at throat

It can be seen from the above figures that:

- While the temperature of gases at throat was 3264 K, the convective heat transfer coefficient was 2500 W/m^{2}K, after (1 s.) the temperature at the internal surface was 1000 K, and after (7 s.) the temperature at the internal surface was 1923 K.
- The temperature decreased gradually through the graphite from internal surface to distance 0.03 m, then decreased sharply until reaching the initial temperature.
- While the temperature of gases at exit was 2150 K, the convective heat transfer coefficient was 900 W/m^{2}K, after (1 s.) the temperature at the internal surface was 500 K, and after (7 s.) the temperature at the internal surface was 1323 K.
- The temperature decreased sharply across the wall thickness at exit until reaching 293K at distance 0.006 m.

4.2. Thermo-structural analysis results

The results of structural analysis due to pressure and thermal loads are presented in Figs.15, 20. The Von Misses stress distribution at time 1 second is presented in Fig.15; The Von Misses stress distribution at time 7 second is presented in Fig.16. Axial, radial and Von Misses stresses through entrance, throat, and exit are obtained.

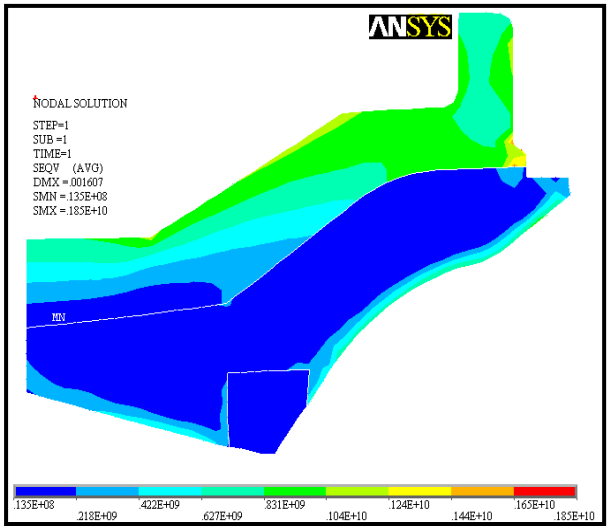

Fig.15 Von Misses stress at time (1 s)

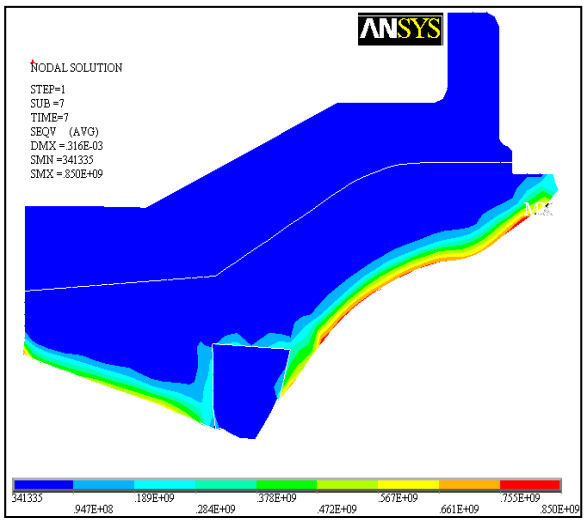

Fig.16 Von Misses stress at time (7 s)

Figure 17 shows the axial, radial, and Von Misses stresses at the entrance section at time (1s), it can be seen that:

- Stresses at internal nozzle wall is more than 700 MPa, this can give an indication about how much the thermal load may influence the nozzle structure.
- stresses decreased gradually in composite, and almost vanishes at distance 0.01 m from the internal surface.
- The axial stress is having the most effectiveness in equivalent stresses than the radial stresses.
- Von Misses stress appear as tension stress at the internal surface then compression stress appears from 0.01m to the steel part.

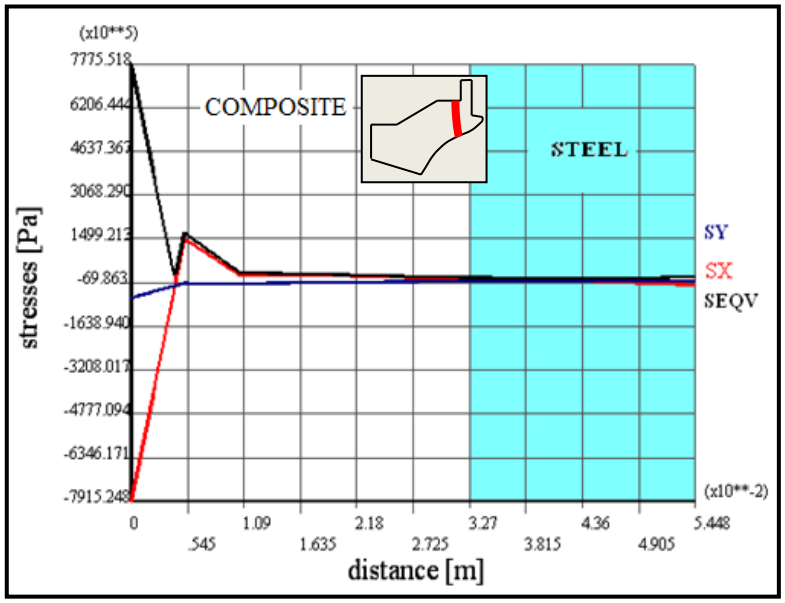

Fig.17 Axial, radial, and Von Misses stresses at time (1 s)

Figure 18 shows the axial, radial, and Von Misses stresses at exit section at (1 s), it can be seen that:

- An elevated value of tension stresses (790 MPa) at the internal surface is seen then decreased through the composite.
- The stresses at the beginning of steel part (0.002 m) increased but with very small value.
- With the increase of time of operation the stresses at the interface between steel and composite increased.
- The radial stresses is lower than axial stresses.

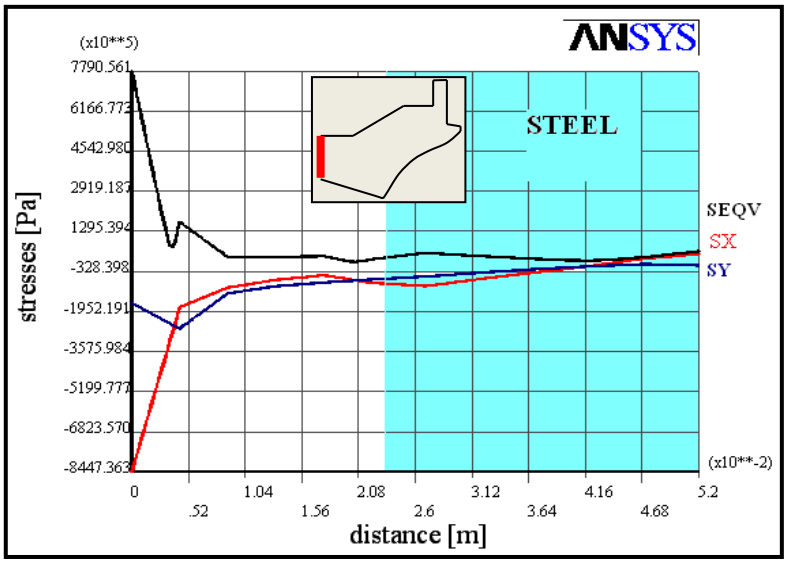

Fig. 18 Axial, radial, and Von Misses stresses at time (1 s)

Figure 19 shows the axial, radial, and Von Misses stresses at the entrance section at time (7 s), it can be seen that:

- The thermal stresses increased with more time of operation.
- The stresses begins to increase in composite part at a distance of 0.01 m with slow rate to became 100 MPa at distance 0.03 m from the internal surface, stresses then began to increase sharply at the interface with the steel due to the rigidity of steel (elasticity of steel is lower than that of composite material).
- Stresses continue to increase in steel to reach 940 MPa at distance 0.038 m then decreased slowly to the outer surface.

Figure 20 shows the axial, radial, and Von Misses stresses at the throat section at time (7 s), it can be seen that:

- Due to very high thermal conductivity of graphite the temperature grows quickly in the graphite section and the thermal stresses caused by the difference in temperature were disappeared.
- Stresses then began to increase in composite part slowly to reach 180MPa at the end of that section.
- Stresses increased sharply in steel section to reach 1059 MPa at the outer surface.
- The difference in slope of increasing of stresses can be clearly seen between composite material and steel due to the change in elastic properties.

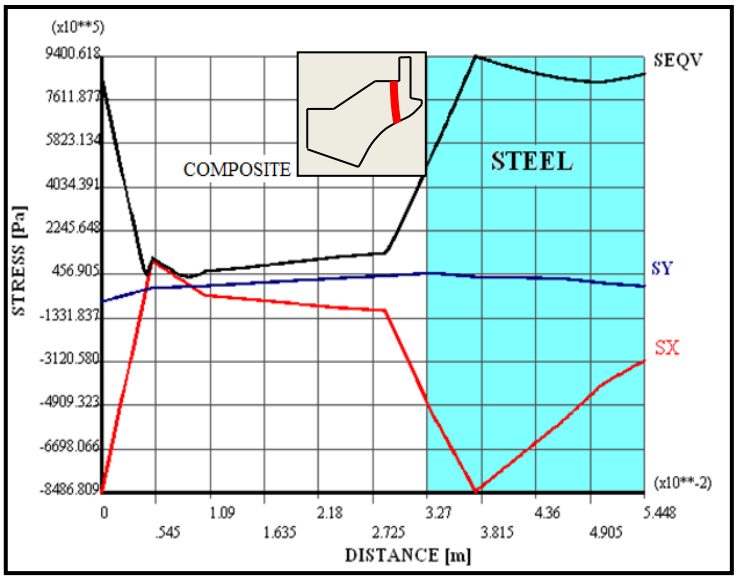

Fig. 19 Axial, radial, and Von Misses stresses at entrance

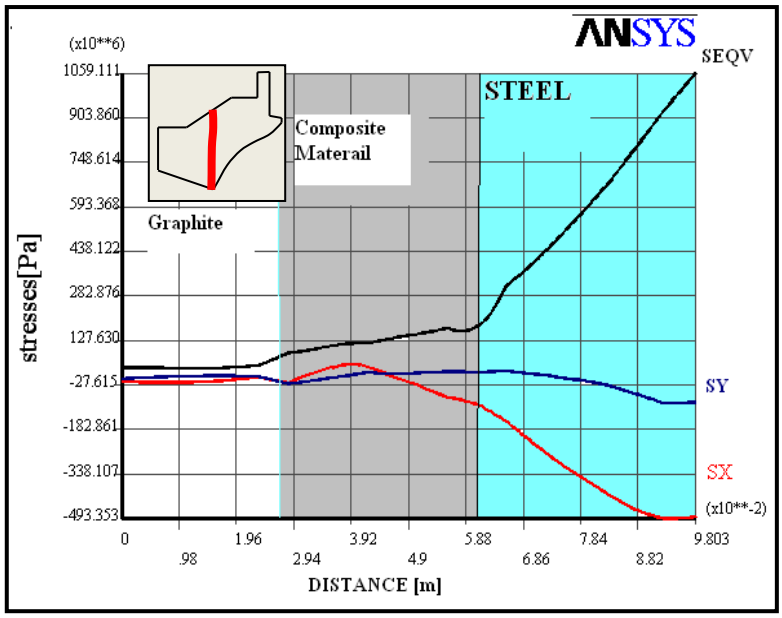

Fig. 20 Axial, radial, and Von Misses stresses at throat section

5. Conclusions

- The difference in temperature behavior across the wall thickness can be realized from the above figures; due to the very high thermal conductivity of graphite the distance affected by the temperature is 7 times as in the entrance and exit sections where the thermal conductivity of the composite material was very low.
- The convictive heat transfer coefficient has a great effect on the temperature transferred to the nozzle wall.
- Thermal loads have a great effect in generating a huge amount of stresses on the nozzle structure (more than 60% from the total stresses on the nozzle).
- The stresses induced at time 1 second give an indication about the necessity of analysis in the beginning of operation to know the effect of thermal shock.
- The effect of thermal stress is increased and can be considered as the main applied load with increasing of time.

- Stresses increase rapidly in steel with a maximum value in steel due to the higher value of elastic modulus than the composite material.
- At the critical section, the maximum value of stresses in the first second is at the interface between the graphite and the composite material, but the maximum value in the last second is at the steel(in the 1 second the thermal load effect did not reach to the steel yet).
- At the beginning of operation time, the maximum stresses occurred at the composite materials, but at the end of firing the maximum stresses occurred in the steel part.
- The maximum value of stresses for the applied nozzle is reached at throat and the entrance section at the end of duration time.
- Using of combined (composite -steel) nozzle to withstand the combined load (thermo-structural), composite used to carrying the thermal load and the steel serve as the main framework carrying structure load.

References

[1] N. Mukherjee and P. K. Sinha, "Thermostructural Analysis of Rotationally Symmetric Multidirectional Fibrous Composite Structures", Computers and Structures, Vol. 65, No. 6, pp. 809-817, 1997.

[2] A-N. Zayed, "Thermo-Structural Analysis of Rocket Nozzle", M. Sc. Thesis, Military Technical College, Cairo, Egypt, 1990.

[3] E.V. Morozov, J.F.P. Pitot de la Beaujardiere, "Numerical Simulation of the Dynamic Thermostructural Response of a Composite Rocket Nozzle Throat", Composite Structures, 2009.

[4] Francisco Alhama, Antonio Campo, "Network Simulation of the Rapid Temperature Changes in the Composite Nozzle Wall of an Experimental Rocket Engine During a Ground Firing Test", Applied Thermal Engineering, Vol. 23, pp. 37-47, 2003.

[5] F. K. Chang and Z. Kutlu, "Strength and Response of Cylindrical Composite Shells Subjected to Out-of-Plane Loading ", J. of Composite Materials, Vol.23, pp 11-31, 1989.

[6] Tsung-Chien Chen, Chiun-Chien Liu," Inverse Estimation of Heat Flux and Temperature on Nozzle Throat-Insert Inner Contour", International Journal of Heat and Mass Transfer, Vol. 51, pp. 3571-3581, 2008.

[7] Vandenboom M, Heister SD. Application of advanced materials in a composite rocket nozzle. In: Proceedings of 34th AIAA/ASME/SAE/ASEE joint propulsion conference and exhibit. Cleveland, USA; 1998.

[8] Cozart AB, Shivakumar KN. Stress analysis of a 3-D braided composite ablative nozzle. In: Proceedings of 40th AIAA/ASME/ASCE/AHS/ASC structures, structural dynamics, and materials conference and exhibit, AIAA/ASME/AHS adaptive structures forum and AIAA forum on non-deterministic approaches. St. Louis, USA; 1999.

[9] Yoo JS, Cho IH, Kim CG. Thermoelastic analysis of a kick motor nozzle incorporating spatially reinforced composites. J Spacecraft Rocket 2003;40(1):83–91.

[10] R.Ramesh Kumar, G.Vinod, S.Renjith, G.Rajeev, M.K.Jana, R.Hrikrishnan, "Thermo-structural analysis of composite structures", Materials Science and Engineering A 412, pp. 66–70, 2005.

[11] Timoshenko, S. and Goodyear, J.N., 1970. “Theory of elasticity”, 3rd edition, McGraw-Hill, New York.

[12] "Metals Handbook: Properties and Selection", Vol. 1, 10th Edition, ASM International, ISBN 0-87170-377-7, 1990.

[13] S.Timoshenko, S.Woinowsky-Krieger, “Theory of plates and shells”, 2nd Ed., MCGRAW-Hill Book Company.